PHYSICAL REVIEW A VOLUME 15, NUMBER 2 FEBRUARY 1977

Total charge-transfer cross sections for H^+, H_2^+, H_3^+, He^+, N^+, N_2^+, Ne^+, Ar^+, Kr^+, and Xe^+ incident on Cs†

F. W. Meyer, C. J. Anderson, and L. W. Anderson
Department of Physics, University of Wisconsin, Madison, Wisconsin 53706
(Received 21 September 1976)

The total cross section for electron capture has been measured for H^+, He^+, N^+, Ne^+, Ar^+, Kr^+, and Xe^+ incident on a Cs vapor target. The energy range investigated was 40–120 keV for incident protons, 30–140 keV for incident N^+, and 20–200 keV for the incident noble-gas ions. Also measured was the total attenuation cross section for H_2^+, H_3^+, and N_2^+ incident on Cs in the energy range 30–160 keV. These attenuation cross sections result from either electron capture or breakup of the incident molecular ion. At velocities below 5×10^5 m/sec, the various cross sections are different both in magnitude and velocity dependence. In the velocity range $(0.5\text{–}1.5)\times10^6$ m/sec, the cross sections for the various incident ions are almost completely independent of the identity of the incident ion. At velocities above 1.5×10^6 m/sec, the individual cross sections are different from one another again. The behavior of the measured cross sections is discussed in terms of a theoretical model for near-resonant charge transfer.

I. INTRODUCTION

Charge-transfer reactions for ions incident on a Cs vapor target have been studied extensively in recent years. The total electron-capture cross section σ_{+0} has been measured for incident hydrogen ions,[1–5] and for incident rare-gas ions.[6–12] These experiments have been carried out with incident ion energies below 40 keV, with the exception of the measurements of Il'in *et al.*,[2] who measured σ_{+0} for H^+ incident on Cs at energies up to 180 keV. In this paper we report measurements of the total electron-capture cross section σ_{+0} for the noble-gas ions incident on Cs with an energy in the range 20–200 keV, for N^+ incident in the energy range 30–140 keV, and for H^+ incident in the range 40–120 keV. We also report measurements of the total attenuation cross section for H_2^+, H_3^+, and N_2^+ incident on Cs with energies in the range 30–160 keV. These attenuation cross sections result from either electron capture or breakup of the incident molecular ion.

Our results show that at incident ion velocities below 5×10^5 m/sec, the individual cross sections are widely different in magnitude and velocity dependence. In the velocity range $(0.5\text{–}1.5)\times10^6$ m/sec, the cross sections are practically identical in magnitude and velocity dependence. At velocities above 1.5×10^6 m/sec, the cross sections are again different in magnitude and velocity dependence. These results are described in greater detail in Sec. II. An interpretation of our measurements using a theoretical model for near-resonant charge transfer is presented in Sec. III. This model is appropriate for use with our measurements, since for all the reactions studied, the dominant process for incident ion velocities below 1.5×10^6 m/sec is the near-resonant capture by the incident ion of the (6*s*) valence electron of a Cs target atom to form a fast neutral atom in an excited state. As discussed in Sec. III, at velocities below 5×10^5 m/sec, the near-resonant capture cross sections depend on the behavior of the molecular potential curves of the reactant and product states at the internuclear separations where charge transfer occurs. At higher velocities the electron-capture cross sections become quasiresonant, and are no longer sensitive to the detailed behavior of the potential curves. When the incident ion velocities become comparable in magnitude to the classical orbital velocities of the target atom core electrons, capture by the incident ion of a Cs atom core electron becomes the dominant process. In the case of the molecular ions incident on Cs at high velocities, the process of dissociative excitation (e.g., $H_2^+ + Cs \rightarrow H_2^{+*} \rightarrow H^+ + H^0$) and dissociative ionization (e.g., $H_2^+ + Cs \rightarrow 2H^+ + e^-$) must be considered in addition to electron transfer.

II. CROSS-SECTION MEASUREMENTS

An accelerator with an acceleration voltage variable from 20 to 250 kV was used for these measurements. A duoplasmatron ion source produces the ion beam. The beam is extracted using a Pierce geometry and is focused by an einzel lens. A 14-section tube accelerates the beam to the desired energy. After momentum analysis and collimation by two 1.5-mm apertures separated by 1 m, the ion beam passes between two parallel plates to which a voltage can be applied. The proper electric field between these plates can deflect the beam into a suppressed Faraday cup located off the beam axis. When the plates are grounded, the ion beam passes between the plates undeflected

and enters the Cs target. The beam emerging from the Cs target contains positive and negative ions as well as fast neutral atoms. A magnet deflects the positive and negative ion beams into two suppressed Faraday cups, one cup for positive ions and the other for negative ions. The cups are located symmetrically to the left and right of the beam axis at $\pm 4^\circ$ with respect to the center of the magnetic deflection field. The neutral beam emerging from the target passes straight through the magnetic field and strikes a Cu metal surface, ejecting electrons. A positively biased ring collects the ejected electrons. The Cs target chamber is 23.2 cm long. In order to reduce the flow of Cs from the target, 0.74-cm i.d. tubes, 7.7 cm long, are used for the entrance and exit apertures of the target. A cooled Cu-cylinder coaxial with the beam axis condenses the Cs vapor that escapes from the entrance and exit tubes. The Cs density increases linearly from nearly zero to the density inside the target as one goes from the end of either the entrance or exit tube into the target. The Cs density is constant in the Cs target. The Cs target thickness π in atoms/cm^2 is given by $\pi = nl$ where n is the Cs density in atoms/cm^3 in the target and l is equal to the length of the target plus one half the length of the entrance tube plus one half the length of the exit tube. The Cs reservoir is located directly below the Cs target and is connected to the target by a 2.54-cm-diam tube. The Cs density in the target is varied by changing the temperature of the Cs reservoir. The Cs target chamber is kept at a constant temperature of ~200 °C which is about 75 °C above the highest reservoir temperatures reached during our measurements. Condensation of Cs in the target chamber is thus avoided. The Cs density in the target is determined by a hot wire gauge located inside the target. The gauge has a guard ring geometry so that the length of the hot wire from which Cs ions are collected is well determined. With the assumption that every Cs atom that hits the hot wire is ionized, the current drawn by the gauge is $I = (\frac{1}{4}n\bar{v})(2\pi rle)$ where n is the Cs target density in atoms/cm^3, $\bar{v}$ is the average Cs atom speed, r is the radius of the hot wire, l is the length of the hot wire, and e is the electronic charge. By measuring I one thus obtains n from $n = (2I)/(\pi\bar{v}rle)$.

The cross sections are measured as follows. An ion beam is extracted from the ion source and accelerated to the desired velocity, momentum-analyzed, and collimated. The intensity of the ion beam incident on the target is measured by deflecting the beam into the suppressed Faraday cup before the target. The current measured is $I_s = N_s e$, where N_s is the number of positive ions incident per sec and e is the electronic charge. The incident ion beam is then permitted to enter the Cs target. The positive ions emerging from the target are deflected by a magnetic field into a suppressed Faraday cup. The current measured is given by $I_+ = N_+ e$ where N_+ is the number of positive ions per sec emerging from the target. When the target thickness π is very small, the ratio I_+/I_s is given by $I_+/I_s = T(1 - \pi\sigma)$, where T is the fraction of the incident positive beam transmitted through the target when $\pi = 0$ and σ is the total cross section to remove a positive ion from the beam by collision with a Cs atom (i.e., the total attenuation cross section). The transmission of our beam through the target at zero target thickness was above 99% (i.e., $T > 0.99$) at all the energies studied. Thus the loss of beam because of misalignment of our apertures or by deflection due to stray electric or magnetic fields is very small.

The total attenuation cross section σ is equal to the sum of the cross sections for the different processes that will remove an ion from the positive ion beam that enters the detector Faraday cup. The processes that can remove a positive ion from the detected beam are charge transfer and elastic scattering through an angle large enough to cause the scattered particle to completely miss the detector Faraday cup. In the case of H_2^+, H_3^+, and N_2^+ incident on Cs, breakup of the incident molecular ion is an additional process that will remove the ion from the detected beam.

We believe that the contribution of the elastic scattering cross section to the total cross section σ is negligible for the following reason. The profile in the horizontal plane of the positive ion beam emerging from the target at the highest densities reached during our cross-section measurements was determined by sweeping the beam across the suppressed Faraday cup in the detection chamber. The Faraday cup subtends an angle of 1.5° as seen from the center of target. At all the energies investigated, the collected ion current was found to be independent of the magnetic deflection field for changes as large as ±10% from the value required to center the beam in the Faraday cup. The ion current drops sharply outside this range of deflection fields as the beam completely misses the cup. This indicates that the angular divergence of the positive ion beam emerging from the target is much smaller than the angle intercepted by the Faraday cup. We therefore conclude that elastic scattering is a negligible loss mechanism for the positive ion beam.

The charge-changing reactions that can remove a positive ion from the beam are single-electron capture, double-electron capture, or the stripping of one or more electrons from the incident ion. We monitor the negative-ion yields, and in all

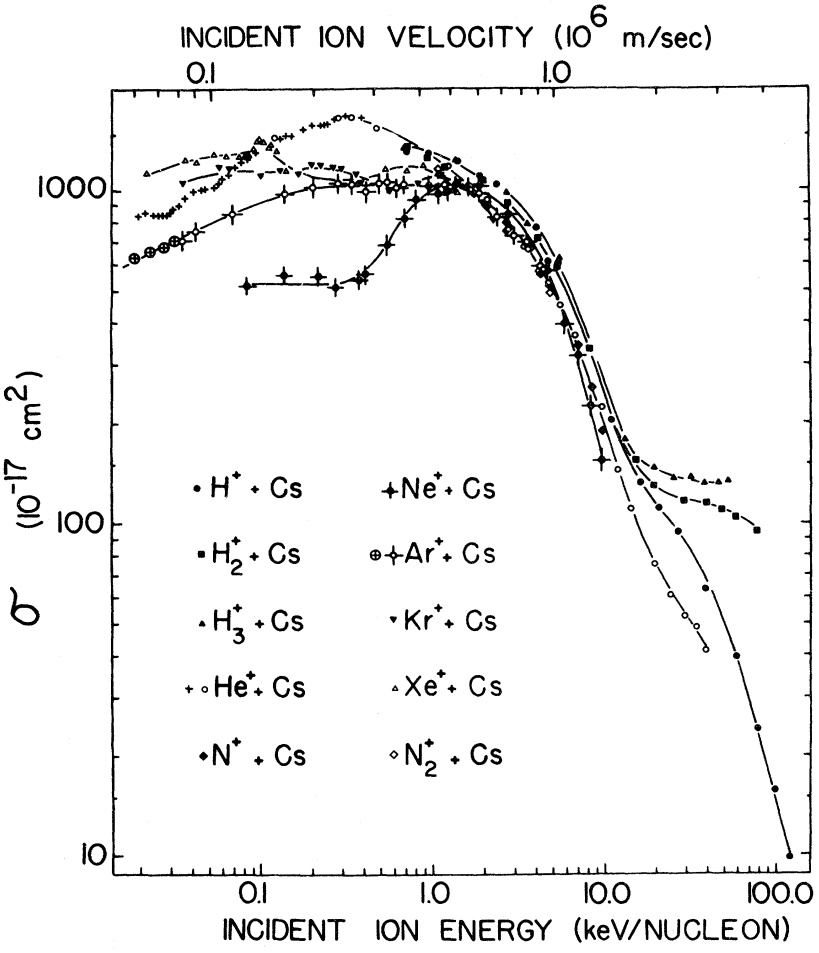

FIG. 1. Total attenuation cross sections σ for hydrogen atomic and molecular ions, nitrogen atomic and molecular ions, and noble-gas ions incident on Cs as a function of the energy per nucleon. The low-energy He^+ and Ar^+ data (+ and ⊕) are taken from Ref. 6.

cases when $\pi < 10^{13}$ atoms/cm^2, the negative-ion production is extremely small compared to the attenuation of the positive beam. For He^+, N^+, Ar^+, Ne^+, Kr^+, or Xe^+ incident it is possible to strip one or more electrons from the ion. The resolution of our charge analyzer was sufficiently high to allow us to resolve singly and doubly charged ions entering the detection chamber. Periodic checks for multiply charged ions performed by sweeping the charge-analyzing field showed no measurable positive beam components aside from the singly charged one. This is reasonable since the stripping cross sections for positive ions incident at the energies investigated are quite small compared to the single-electron-capture cross sections. Thus for H^+, He^+, N^+, Ne^+, Ar^+, Kr^+, or Xe^+ incident on a Cs target $\sigma \simeq \sigma_{+0}$, and for H_2^+, H_3^+, or N_2^+ incident on a Cs target $\sigma \simeq \sigma_{+0} + \sigma_D$, where σ_D is the cross section for dissociative excitation or dissociative ionization of the molecular ion (i.e., σ_D is the cross section for breakup of the molecular ion into one or more atomic ions).

At a given energy we measure I_s and I_+ as a function of π for sufficiently low values of π, that the ratio I_+/I_s is a linearly decreasing function of π. The intercept at $\pi = 0$ gives T and the slope of I_+/I_s as a function of π gives $-T\sigma$. We use the neutral detector as a check that the values of π are small enough so that the fractional yield of the neutrals is increasing linearly, and we use the negative detector to verify that the negative yields are very small.

The results of our measurements of the various cross sections are shown in Fig. 1, and summarized in Table I. Previously reported measurements[5,6,10-12] of cross sections for incident ion energies below 40 keV are also shown in Fig. 1. The uncertainties quoted in Table I result primarily from two sources: (i) random errors in the current measurements, and (ii) the systematic uncertainty in the Cs density determination using the surface ionization detector inside the target. The error due to (i) is about ±8% at most energies, and that due to (ii) is estimated to be about ±5%.

TABLE I. Total attenuation cross sections $\sigma(10^{-17}\ \mathrm{cm}^2)$ for hydrogen atomic and molecular ions, nitrogen atomic and molecular ions, and noble-gas ions incident on Cs as a function of the beam energy (keV).

Beam energy	H^+	H_2^+	H_3^+	He^+	N^+	Ne^+	N_2^+	A^+	Kr^+	Xe^+
20										1140 ± 83
30					881 ± 68		1094 ± 93	1074 ± 66	1065 ± 58	
40	63 ± 4	128 ± 9	177 ± 13	225 ± 13	820 ± 55	1065 ± 57				
50				144 ± 17	695 ± 58		993 ± 70	1037 ± 58	1001 ± 56	1057 ± 60
60	40 ± 4	116 ± 7	147 ± 8	110 ± 7	599 ± 37	854 ± 47	909 ± 100			
70					531 ± 46					
75								983 ± 59	1063 ± 58	1154 ± 64
80	24 ± 2	114 ± 8	135 ± 8	75 ± 6	433 ± 28		777 ± 70			
100	16 ± 2	108 ± 7	138 ± 8	60 ± 4	328 ± 29	576 ± 34	698 ± 66	831 ± 59	1125 ± 61	1145 ± 60
120	10 ± 2	103 ± 6	131 ± 11	53 ± 4	254 ± 19		599 ± 35			
125						400 ± 22		736 ± 42	1052 ± 60	1197 ± 64
140			131 ± 9	48 ± 4	191 ± 15		516 ± 52			
150						319 ± 21		706 ± 39	1020 ± 67	1127 ± 65
160		93 ± 6	133 ± 9	42 ± 3						
175						227 ± 21			925 ± 75	999 ± 60
180								590 ± 36		
195										989 ± 65
200						155 ± 11			813 ± 50	

The overall errors as given in Table I are typically ±10%. The cross sections measured in the present work are in excellent agreement with our low-energy cross-section measurements[5,10–12] in the energy range 20–40 keV, where the measurements overlap. We also note that our previously reported cross sections for He^+ and Ar^+ incident on Cs[11,12] are in excellent agreement with the measurements of Peterson and Lorents[6] where the two sets of measurements overlap.

As has already been pointed out, Il'in *et al.*[2] have measured the electron-capture cross section for H^+ incident on Cs in the energy range 10–180 keV. In the energy range investigated in the present work, the cross sections of Il'in *et al.* have the same velocity dependence as our measurements, but are consistently 25% larger than our cross sections. Il'in *et al.* estimate a systematic uncertainty of 20% for their cross-section measurements.

As is apparent from Fig. 1, there are three ranges of the incident ion velocity, each of which appears to be characterized by a particular behavior of the cross sections taken as a whole. For velocities of the incident ion less than 5×10^5 m/sec (i.e., for energies per nucleon below 1 keV/nucleon), the various cross sections differ greatly among themselves both in magnitude and velocity dependence. We call this region I. As the energy per nucleon of the incident ions is increased beyond 1 keV/nucleon, there is a striking change in the behavior of the cross sections. For velocities of the incident ion in the range $(0.5–1.5) \times 10^6$ m/sec (i.e., energies per nucleon in the range 1–10 keV/nucleon), the electron-capture cross sections are almost completely insensitive to the identity of the incident ion, and all the cross sections are nearly the same in magnitude and velocity dependence. We call this region II. For velocities of the incident ion greater than 1.5×10^6 m/sec (i.e., for energies per nucleon greater than 10 keV/nucleon, the cross sections for the various incident ions become different again, although they all share the common feature of decreasing more slowly with increasing velocity than in region II. We call the region of velocities greater than 1.5×10^6 m/sec region III.

III. INTERPRETATION OF THE EXPERIMENTAL MEASUREMENTS

In regions I and II, the charge-transfer processes for all the reactions investigated have several features in common. The Cs electron captured by the incident ion to form a fast neutral is the valence (6s) electron. All the projectile species investigated have neutral excited states with ionization energies quite close to the ionization potential of Cs. Consequently, for any of the incident ions X^+ investigated, there exist final states $(X^* + Cs^+)$ that lie very close in energy to the initial state $(X^+ + Cs)$. The electron-capture cross sections are usually large for those reactions that have a small energy defect, i.e., that have a small energy difference between the reactant and product states. The fast neutrals are thus formed preferentially in these near-resonant excited states. The charge-transfer reactions are therefore predominantly near-resonant reactions. For the heav-

ier rare-gas ions[11,12] and the molecular ions incident on Cs, the number of near-resonant final states is large.

The charge-transfer cross sections can be discussed in terms of the model for near-resonant charge transfer proposed by Rapp and Francis,[13] Demkov,[14] and Olson.[15] The mechanism for electron capture in this model is the interaction between close-lying potential curves of the reactant and product states at large internuclear separations. In this model for near-resonant charge transfer, the interaction matrix element is taken as $e^{-\lambda R/a_0}$, where R is the internuclear separation, λ/a_0 is an empirical parameter inversely proportional to the radius of the participating electron orbitals, and a_0 is the radius of the first Bohr orbit. The parameter λ is usually taken to be equal to $(I/I_H)^{1/2}$, where I is an "appropriate" mean of the effective ionization potentials of the initial and final neutral atoms in the reaction,[13] and I_H is the ionization potential of hydrogen. Since the final state of the neutral atom or molecule produced in region I or II has nearly the same ionization potential as Cs, the value of I is approximately equal to 3.9 eV for all the reactions; λ is therefore equal to about 0.54 for all the reactions studied. In the above model, charge transfer occurs at an internuclear separation of the incident ion and target atom, R_c, for which the interaction matrix element equals one half the energy separation of the initial and final state potential curves, $\Delta V(R_c)$. At low velocities, the charge-transfer probability, and consequently the charge-transfer cross section, is a function of R_c, $\Delta V(R_c)$, λ, and v, the relative velocity of the incident ion-target atom system.[15] At small velocities, therefore, the charge-transfer cross sections depend on the behavior of the molecular potential curves of the reactant and product states near $R=R_c$. At the large internuclear separations involved, the behavior of the reactant and product potential curves as R decreases from infinity to R_c is determined by the dipole polarizabilities, and quadrupole moments of the participating neutral atoms.[15] Since the fast neutral atoms produced by charge exchange from the various incident ions have different dipole polarizabilities and quadrupole moments, the internuclear separation R_c, where the charge transfer occurs, as well as the energy separation $\Delta V(R_c)$, will be different for the various incident ions. For this reason, the various cross sections are different in region I. Also contributing to the variations among the various cross sections may be the different number of near-resonant product channels available to the various reactions.

For region II the situation is markedly different than for region I. We find experimentally that in this velocity range all the cross sections are closely similar in velocity dependence and magnitude. This striking behavior is anticipated in the theoretical model for near-resonant charge transfer.[13–15] For sufficiently high velocities, i.e., for sufficiently short collision times, the energy uncertainty becomes large compared to the energy separation of the reactant and product potential curves. As a result, equal mixing of the two states occurs. The probability for charge transfer consequently is independent of R_c and $\Delta V(R_c)$, and becomes formally identical to that for symmetric resonant charge transfer. The cross sections for near-resonant electron capture in the high-velocity limit therefore depend only on the parameter λ, and on the relative velocity. We refer to this behavior of the cross sections at high velocities as quasiresonance. Because each of the reactions studied has a small energy defect (<1.0 eV), all the reactions have nearly the same values of $\lambda(\simeq 0.54)$. Therefore all the cross sections in region II have nearly the same value at a given velocity.[16]

The velocity at which the charge-transfer reactions become quasiresonant depends on the magnitude of the energy defects of the reactions. The larger the energy defects, the greater the velocity at which the transition to quasiresonance occurs.[13] Rapp and Francis calculate that for energy defects between 0.5 and 1.0 eV (which includes the reactions of the present study in region II), this transition occurs at velocities between 4×10^5 and 6×10^5 m/sec. This prediction is in excellent agreement with our measurements, which indicate that at velocities above 5×10^5 m/sec, quasiresonance has been reached for all the reactions studied.

The cross sections for the various reactions studied are nearly the same up to velocities of about 1.5×10^6 m/sec. For velocities above 1.5×10^6 m/sec, the individual cross sections are once again different in magnitude and velocity dependence. In Fig. 2 a semilog plot of the cross sections at velocities above 5×10^5 m/sec clearly shows this transition. As can be seen from Fig. 2, in region III the measured cross sections decrease more slowly with increasing velocity than in region II. We believe that this "flattening out" of the cross sections at higher velocities (region III) may be due to the increased participation of the Cs core electrons in the charge-transfer reactions, as the incident ion velocities approach those of the Cs core electrons. A number of theoretical calculations of the total charge-transfer cross section for protons incident on alkali-metal vapor or noble-gas atom targets[17–20] show that the magnitudes and velocity dependences of these cross sections at high velocities (>2×10^6 m/sec) may be

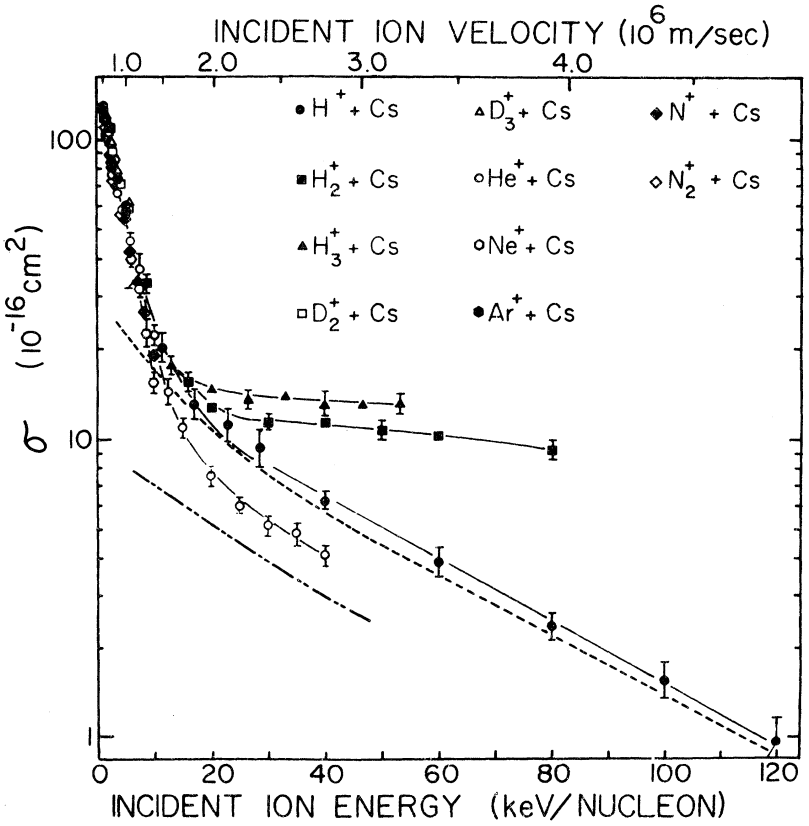

FIG. 2. Total attenuation cross sections σ for hydrogen atomic and molecular ions, nitrogen atomic and molecular ions, and noble-gas ions incident on Cs. ----, the total electron-capture cross section for $H^+ + Xe$ from Ref. 21; — — —, the total electron-capture cross section for $He^+ + Ar$ from Ref. 17.

understood if allowance is made for capture of target atom core electrons. Vinogradov *et al.*,[18] for example, calculate that for protons incident on Cs in the energy range 20–40 keV, the $(5p)^6$ electrons contribute 70%, and the $(5s)^2$ electrons 30% to the total charge-transfer cross sections. The importance of the Cs core electrons in charge exchange at high velocities is further demonstrated by the experimental fact that at higher velocities, the total electron-capture cross sections for a given ion incident either on an alkali-vapor target or on a target of noble-gas atoms with the same electron configuration as the alkali-metal core, are quite similar in magnitude and dependence on the velocity.[2] In Fig. 2 we show the high-energy cross sections for H^+ incident on Xe, measured by Afrosimov *et al.*[21] The Xe atom has the same electron configuration as the Cs core. The cross sections are almost identical at velocities above 1.5×10^6 m/sec. Since the energy defects for the capture by an incident proton of a $(5p)^6$ Xe electron ($\Delta E = -1.4$ eV), and that of a $(5p)^6$ Cs core electron ($\Delta E = 3.6$ eV) to produce H(1*s*) are substantially different, it might be objected that the above comparison lacks meaning. Calculation shows, however, that at velocities greater than 1.5×10^6 m/sec, both reactions are quasiresonant, i.e., independent of the energy defects of the reactions.[13] The two cross sections therefore merely scale, roughly as $(a_0/\lambda)^2$, the "size" of the participating electron shells.[22] For reactions having energy defects that are not small compared with the ionization potentials of the initial and final neutral states, the value of λ is somewhat arbitrary.[13] We therefore use the tabulated Hartree-Fock calculations of Herman and Skillman[23] in estimating the "sizes" of the $(5p)^6$ shells of Xe and Cs. These calculations show that the electron distribution functions of the $(5p)^6$ shells of Xe and Cs peak at $r = 1.93a_0$ and $1.77a_0$, respectively. On this basis the $H^+ + Xe$ cross section data would overestimate the contribution of the Cs core to the total charge-transfer cross section by less than 20%.

Participation of the Cs core electrons for He^+ incident on Cs may be inferred by comparison of this cross section with that for He^+ incident on Ar, measured by Barnett and Reynolds,[24] and also shown in Fig. 2. This reaction is quasiresonant at velocities above 2×10^6 m/sec, as is the reaction for electron capture of one of the $(5p)^6$ electrons of Cs, forming a fast He atom in the $1\,^2S$ state. The scaling suggested by Rapp and Francis may therefore be used to estimate the difference between the two cross sections due to the different

target "sizes" for the two reactions. Using tabulated Hartree-Fock calculations as described in the previous case, it is estimated that the $He^+ + Ar$ cross sections underestimate the Cs core contribution for He^+ incident by about 25% at all velocities above 2×10^6 m/sec. From Fig. 2 we see that the $He^+ + Ar$ cross section above 2×10^6 m/sec indeed lies roughly 25% below our measured $He^+ + Cs$ cross section. We conclude that capture of a Cs core electron is probably the dominant process at high velocities for He^+ incident on Cs just as it is for H^+ incident on Cs.

R. E. Olson has suggested charge transfer via rotational coupling on the repulsive wall of the Σ reactant state potential curve with a Π product state as an alternative mechanism that might lead to the weakened velocity dependence of the cross section in region III.[25] No detailed calculations have been performed to date to determine the contribution of rotational coupling to the total charge-transfer cross sections at higher velocities for any of the reactions we have studied.

As pointed out earlier, the cross sections measured in the present experiments are actually the total attenuation cross sections for loss of an incident ion from the beam that reaches the final detector Faraday cup. In the case of the atomic ions incident on Cs, this loss cross section is closely equal to the single-electron capture cross section, since at the energies investigated, single-electron capture is by far the most important mechanism for the loss of an incident ion. In the case of the molecular ions H_2^+ and H_3^+ incident on Cs, however, the exceedingly weak velocity dependence of the loss cross sections at velocities above 1.5×10^6 m/sec suggests that at these higher velocities, additional mechanisms play an important role in the loss of the incident molecular ions.

For H_2^+ incident on Cs, the reactions leading to loss of the incident ion are as follows:

$$H_2^+ + Cs \rightarrow H_2^{0*} + Cs^+, \quad (1)$$

$$H_2^+ + Cs \rightarrow H_2^{+**} \ (\text{e.g.}, 2p\sigma_u) \rightarrow H^+ + H^0, \quad (2)$$

$$H_2^+ + Cs \rightarrow 2H^+. \quad (3)$$

Similar reactions may be written for H_3^+ or N_2^+ incident on Cs. For the molecular ions incident on Cs at low velocities, electron capture (1) is the dominant loss mechanism, analogous to the case of the incident atomic ions. Included in reaction (1) is the possibility of dissociation resulting from capture into, e.g., the $a\,^3\Sigma_g^+$ state, followed by radiative decay to the repulsive $b\,^3\Sigma_u^+$ state. The electron capture (1) is a near-resonant process and is important in regions I and II. On the other hand, dissociative excitation (2) or dissociative ionization (3) requires an interaction with the tightly bound

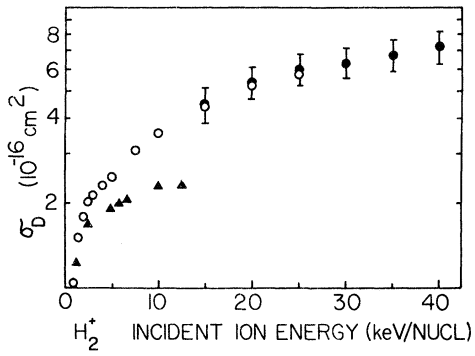

FIG. 3. Total cross section for dissociative excitation or dissociative ionization. Open circles are total cross sections for H^+ production with H_2^+ incident on Xe (Ref. 26); solid triangles are measurements of the same cross section by Morgan *et al.* (Ref. 27); solid circles are the difference between our measured total loss cross sections for H_2^+ and He incident on Cs, respectively.

Cs core electrons in order to obtain the necessary energy transfer (>5 eV). It is reasonable, therefore, that for molecular ions, dissociation by reactions (2) and (3) and electron capture of a Cs core electron both become important mechanisms for the loss of an incident ion at roughly the same velocities.

Although our measurements were not able to determine the relative contributions of dissociative excitation or ionization and electron capture to the loss of the incident molecular ions, we estimate that the partial cross section for H_2^+ incident on Cs due to electron transfer alone is roughly the same as the total charge-transfer cross section for He^+ incident on Cs. Both H_2^+ and He^+ have only a single electron, and thus might be expected to have similar cross sections. The partial cross section due to dissociative excitation or dissociative ionization of the molecular ion is thus estimated to be equal to the difference between the measured cross section for H_2^+ and He^+ incident on Cs, respectively. As can be seen from Fig. 3, this estimate is in good agreement with the measured cross section for H^+ production when H_2^+ is incident on Xe.[26,27] Lack of the appropriate data precludes a similar analysis for the case of H_3^+ incident on Cs. We estimate, however, that dissociation and charge-transfer contribute in roughly the same proportions for H_3^+ on Cs as for H_2^+ incident on Cs. Although reactions similar to (2) and (3) would be important for N_2^+ incident on Cs when the incident ion velocity is greater than 1.5×10^6 m/sec, our measurements do not extend to this velocity range. The only reaction important for N_2^+ incident on Cs is therefore one similar to reaction (1).

IV. CONCLUSIONS

We have measured the total cross sections for electron capture by an incident ion from a Cs vapor target for H^+, N^+, and the noble-gas ions in the intermediate keV energy range. In addition, we have measured the total attenuation cross sections for H_2^+, H_3^+, N_2^+ incident on Cs. At incident velocities below 5×10^5 m/sec there is considerable variation in the behavior of the individual cross sections, reflecting the variations in the potential curves of the reactant and product states at finite separations for the various reactions studied. At velocities in the range $(0.5–1.5)\times10^6$ m/sec, the charge-transfer reactions are quasiresonant. Since, in addition, all the reactions dominant in this region have small energy defects, the various cross sections have very similar magnitudes and velocity dependences. At velocities above 1.5×10^6 m/sec, interaction of the incident ions with the Cs core electrons is the dominant process. At these velocities the reactions involving Cs core electrons are also quasiresonant for the incident ions studied. The energy defects of these reactions are, however, considerably larger than those of the corresponding reactions involving the Cs valence electrons. The parameter $(a_0/\lambda)^2$ characterizing the "sizes" of the participating electron orbitals, therefore differs significantly for the various reactions. It is for this reason that the cross sections for He^+ and H^+ incident on Cs have different magnitudes yet similar velocity dependences at these higher velocities. The exceedingly weak velocity dependence of the attenuation cross sections for H_2^+, and H_3^+ incident on Cs at velocities above 1.5×10^6 m/sec is attributed to to dissociative excitation or dissociative ionization, which was shown to make a significant contribution to the total cross section for loss of the incident molecular ions at velocities above 1.5×10^6 m/sec.

---

†Work supported in part by ERDA Contract No. AT(11-1) Gen.-7.

[1]A. S. Schlachter, P. J. Bjorkholm, D. H. Loyd, L. W. Anderson, and W. Haeberli, Phys. Rev. 177, 184 (1969).
[2]R. N. Il'in, V. A. Oparin, E. S. Solov'ev, and N. V. Fedorenko, Zh. Tekh. Fiz. 36, 1241 (1965) [Sov. Phys.-Tech. Phys. 11, 921 (1967)].
[3]G. Spiess, A. Valance, and P. Pradel, Phys. Rev. A 6, 746 (1972).
[4]W. Gruebler, R. Schmelzbach, V. König, and P. Marmier, Helv. Phys. Acta 43, 254 (1970).
[5]F. W. Meyer and L. W. Anderson, Phys. Lett. 54A, 333 (1975).
[6]J. R. Peterson and D. C. Lorents, Phys. Rev. 182, 152 (1969).
[7]A. S. Schlachter, D. H. Loyd, P. J. Bjorkholm, L. W. Anderson, and W. Haeberli, Phys. Rev. 174, 201 (1968).
[8]B. L. Donnally and G. Thoeming, Phys. Rev. 159, 87 (1967).
[9]J. L. Montmagnon, H. De Palmas, J. P. Grouard, P. Lefebure, and E. Mercier, Phys. Lett. 46A, 227 (1974).
[10]F. W. Meyer and L. W. Anderson, Phys. Lett. 49A, 441 (1974).
[11]F. W. Meyer and L. W. Anderson, Phys. Rev. A 9, 1909 (1974).
[12]F. W. Meyer and L. W. Anderson, Phys. Rev. A 11, 586 (1975).
[13]D. Rapp and W. E. Francis, J. Chem. Phys. 37, 2631 (1962).
[14]Yu. N. Demkov, Zh. Eksp. Teor. Fiz. 45, 195 (1963) [Sov. Phys.-JETP 18, 138 (1964)].
[15]R. E. Olson, Phys. Rev. A 6, 1822 (1972).
[16]We wish to thank Dr. R. E. Olson for pointing out to us why σ_{+0} should be independent of the identity of the incident ion in this velocity range.
[17]R. A. Mapleton and N. Grossbard, Phys. Rev. 188, 228 (1969).
[18]A. V. Vinogradov, L. P. Presnyakov, and V. P. Shevel'ko, Zh. Eksp. Teor. Fiz. Pis'ma Red. 8, 449 (1968) [JETP Lett. 8, 275 (1968)].
[19]V. S. Nokolaev, Zh. Eksp. Teor. Fiz. 51, 1263 (1966) [Sov. Phys.-JETP 24, 847 (1967)].
[20]A. V. Vinogradov and V. P. Shevel'ko, Zh. Eksp. Teor. Fiz. 59, 593 (1970) [Sov. Phys.-JETP 32, 323 (1971)].
[21]V. V. Afrosimov, R. N. Il'in, and E. S. Solov'ev, Zh. Tekh. Fiz. 30, 705 (1960) [Sov. Phys.-Tech. Phys. 5, 661 (1960)].
[22]J. B. Hasted, in *Atomic and Molecular Processes*, edited by D. R. Bates (Academic, New York, 1962).
[23]F. Herman and S. Skillman, *Atomic Structure Calculations* (Prentice-Hall, Englewood Cliffs, N.J., 1963).
[24]C. F. Barnett and H. K. Reynolds, Phys. Rev. 109, 355 (1958).
[25]R. E. Olson (private communication).
[26]J. F. Williams and D. N. F. Dunbar, Phys. Rev. 149, 62 (1966).
[27]T. J. Morgan, K. M. Berkner, W. G. Graham, R. V. Pyle, and J. W. Stearns, Phys. Rev. A 13, 664 (1976).